JOURNAL OF MATERIALS SCIENCE 28 (1993) 225–238

The fibrillar hierarchy in liquid crystalline polymers

L. C. SAWYER, R. T. CHEN, M. G. JAMIESON
Hoechst Celanese Research Division, 86 Morris Avenue, Summit NJ 07901, USA

I.H. MUSSELMAN
Department of Chemistry, University of North Carolina, Chapel Hill, NC 27599, USA

P.E. RUSSELL
Department of Materials Science and Engineering and Precision Engineering Center, North Carolina State University, Raleigh, NC 27695, USA

It is well known that the structure of highly oriented liquid crystalline polymers (LCPs) can be characterized by a hierarchical fibrillar structural model. Structure models were first developed for the lyotropic aramid fibres in the late 1970s and a structural model was developed for the thermotropic copolyesters in the mid-1980s. Recently, imaging techniques with higher potential capability and resolution have been applied to assess the size, shape and organization of microfibrillar structures observed in LCPs. Field emission scanning electron microscopy and scanning tunnelling microscopy permit imaging of regions from 1 nm to many micrometres. As a result, the nature of the microfibrillar hierarchy has been further clarified and the macromolecular size has been shown to be less than 2 nm. The shape of the microfibrils has been shown to be tape-like. The LCP structural model, consisting of elongated well-ordered microfibrils continues to be consistent with measured properties: high anisotropy, very high tensile modulus and strength and poor compressive properties. A more detailed structural model is proposed to describe the macromolecular microfibril size, shape and organization for comparison with polymer composition and mechanical property evaluation.

1. Introduction

The last two decades have seen the vast growth of a new technology in high-performance polymeric materials owing to the invention and development of liquid crystalline polymers (LCPs) [1–10]. The concept of LCPs originated with Onsager [11], Isihara [12] and Flory [13, 14] who treated theories relating to the packing of rigid rod-like molecules. The processing of LCPs in elongational flow fields, in spinning, or in extrusion processes, results in a highly oriented extended chain structure in the solid state [1–6, 10]. These extended chain structures form owing to the flow characteristics of liquid crystals which are dominated by the nematic character in the melt or solution [15–23]. The long relaxation times for LCPs results in their orientation in the melt or solution being "frozen" into the solid state [24]. These highly oriented polymeric materials exhibit impressive mechanical and thermal properties compared to conventional polymers. Study of the complex interactions of liquid crystal chemical structure, in the nematic melt or solution, and their further development during processing to form oriented textures and outstanding physical properties, are currently being investigated in many materials science research laboratories.

Many hundreds of LCP compositions have been documented in review papers and patents [1–10, 25–27], the most commercially important of which fall into two categories.

(a) Lyotropic aramids such as poly(*p*-phenylene terephthalamide) (PPTA), also known as Kevlar, commercialized by duPont (i.e. 8–10, 25–28).

(b) Thermotropic aromatic copolyesters, such as the Eastman-modified polyesters [i.e. 29–33], and the Vectra family of LCP resins and Vectran fibres commercialized by Hoechst Celanese (i.e. [1, 15, 16, 34–40]).

Theoretical models of the LCP solid state structure, as well as those derived from experimental measurements, have value in permitting prediction of LCP structure–property relationships. The now well-known "hierarchies of structure" for LCPs were first described for aramids by Dobb *et al.* [41]. It is now known that the structure of highly oriented LCPs can be characterized by a hierarchical fibrillar microstructure [38–40]. Details of the aramid fibrillar structure have been published by Schaefgen and co-workers [26, 28], Dobb and co-workers [6, 41–45], Sotton [45] and Sawyer and co-workers [38–40]. In addition, documentation of the supramolecular structure of the

0022–2461

skin–core textures in moulded thermotropic articles has been provided by Ide and Ophir [15, 16], Thapar and Bevis [22], Baer *et al.* [47] and Sawyer and coworkers [38–40]. These models are useful for understanding the effect of various fabrication processes on the resulting structures. The models account for microstructures on a scale typically observed in light microscopy (LM) or scanning electron microscopy (SEM), although in our earlier paper [38] structures on a scale of about 10 nm were reported from a transmission electron microscopy (TEM) study. More recently, Sawyer and Jaffe [38] described the first general structural model that included both the aramids and the aromatic copolyesters, of major interest owing to the demonstrated similarities of the lyotropic and thermotropic LCP microstructures. Extensive TEM imaging by Donald and Windle [48–52] revealed banded textures and evidence for aperiodic crystallites (non-periodic layer crystallites, NPL) within oriented thermotropic LCPs formed by shearing on a glass slide [51, 53, 54]. Gutierrez *et al.*, in their X-ray diffraction studies, suggested that the thermotropic LCPs are random in nature although they observed evidence of crystallinity [55].

The elucidation of a hierarchical, microfibrillar structural model [38] included direct study of Vectra mouldings and extrudates as well as Vectran and Kevlar fibres. The model has been extended to other highly oriented materials and has been well accepted as depicting the morphology of the aramid and thermotropic aromatic polyester LCPs. The characterization utilized a broad range of microscopy techniques [38–40], including LM, SEM and TEM as well as X-ray diffraction studies [36, 48, 49, 55]. Although the model provided a description of three levels of fibrillar architecture, the finest such unit, the microfibril, was not observed in much detail. From this study, questions remained regarding the nature of structures less than 10 nm in size.

Recently, imaging techniques with higher spatial resolution have been applied to address questions regarding the size, shape and organization of microfibrillar structures [56, 57]. Field emission scanning electron microscopy (FESEM) at low voltages, and more importantly, scanning tunnelling microscopy (STM), are capable of imaging regions from 1 nm to many micrometres on the same specimen. The experimental observations obtained using these novel characterization techniques have been correlated and compared to results of prior studies and to observations from more traditional imaging methods, such as polarized light microscopy (PLM) and TEM, to aid in the interpretation of structures from the nanometre to the micrometre-size scale.

The present focus of LCP research is to develop a better understanding of the process–structure–property relationships controlling the thermotropic polymers and the aramids, especially in defining the relationships of polymer structure and properties (i.e. tensile modulus and tensile strength). Although it is well known that a higher molecular orientation favours a higher tensile modulus, it is unclear whether this molecular orientation is related to the microfibrillar structure (i.e. the microfibril size and organization of these microfibrils into fibrillar units) and whether such structural studies are useful in predicting mechanical properties.

Theories of LCP organization by Ward and coworkers [2, 58–61] have provided insight into the molecular arrangement of these polymers and the effect of such arrangements on mechanical properties, especially the various moduli. It is important to understand LCP organization and mechanical property relationship as the tensile modulus of the highly oriented LCP fibres approaches theoretical values [1, 38, 62]. The nature of the basic structural unit for the aggregate model, used as a descriptor of the properties in these theories, is not defined and is of major interest to materials science studies.

This paper further delineates the LCP structural model based on observations made using a range of complementary microscopes. The microstructural findings will be compared with the mechanical properties of the LCPs to aid in their development.

2. Experimental procedure

2.1. Materials

The LCPs investigated in this study consisted of highly oriented Vectran (tradename, Hoechst Celanese Corporation) fibres and thin extruded tapes typically composed of naphthalene moiety containing copolyesters [1, 38], i.e. copolyesters composed of 2, 6-naphthyl and 1, 4-phenyl units and other related thermotropic polymers. The aramid fibre, Kevlar (tradename, duPont), was also investigated to compare a lyotropic and thermotropic fibre. Fibres in this study had tensile moduli of about 200–300 GPa, shear moduli of 0.1–1.5 GPa and compressive strengths of approximately 0.35 GPa. The well-known unidirectionally oriented structures of Vectran and Kevlar fibres were revealed previously by X-ray diffraction (e.g. [6, 10, 29, 31, 48–50, 55]) and microscopy (e.g. [6, 22, 35, 38–54, 63]).

2.2. Sample preparation and instrumental methods

Surfaces and internal textures of the highly oriented, thin extruded tapes and fibres were examined by a range of techniques including polarized light microscopy (PLM), field emission scanning electron microscopy (FESEM), TEM and STM. For internal structure study, the LCP samples were prepared by the Scott peel-back technique and by ultrasonication, both of which have been previously described [38–40]. The peel-back method reveals internal structures within the fibres which can be observed by PLM, FESEM and STM. Ultrasonication was used to rupture fibres and tapes into finely textured fibrils and microfibrils for analysis by TEM, FESEM and STM. The fibrils mounted on copper TEM grids were shadowed with Au–Pd by vacuum evaporation to enhance topography and facilitate fibril thickness measurements [40, 56, 57]. Selected-area electron diffraction was also performed on the JEOL 100CX STEM

operated at 100 kV. As in the earlier studies [35, 38, 40], longitudinal ultrathin sections, prepared by ultramicrotomy, were coated with evaporated carbon prior to imaging. To our knowledge, this is the first STM study in which polymers have been prepared using the peel-back and sonication techniques.

LCP samples were mounted on silicon or highly oriented pyrolytic graphite (HOPG) substrates for FESEM and STM studies. The specimens were then coated with ~ 5 nm of platinum using ion-beam sputtering (Ion Tech., Ltd) in a turbo-pumped system, backfilled with ultrapure argon [40, 56, 57, 64]. Ion-beam sputter coatings have been shown to introduce minimal topography to original surfaces as is evident from the measured root mean square surface roughness values of less than 1 nm for these fine-grain platinum coatings [57, 65].

FESEM imaging was conducted in a JEOL 840 field emission scanning electron microscope at an excitation energy of 2–5 kV [56, 57, 65]. All STM images were acquired in air using a Nanoscope II, Digital Instruments, Inc. scanning tunnelling microscope with a long-range tube scanner (D head) which was calibrated by the manufacturer. The software for data acquisition and image processing was also provided by Digital Instruments, Inc. Controlled geometry Pt/Ir tips, formed by a two-step electrochemical etching procedure [65], were used exclusively to acquire images from the LCP samples in order to minimize tip-related image artefacts. The images were acquired in the constant current mode, typically using a 1 nA set current with the sample biased positively 100 mV with respect to the tip. Width and thickness measurements were made of the smallest microfibrils using the software package [56, 57].

3. Results

3.1. Liquid crystal "domains"

Liquid crystal "domains" are regions of local order in which there is correlative nematic order bounded by walls or disclinations [67–70]. The domains have a defined orientation described by a director. Models for the "domain" flow of liquid crystals have been described by Flory [13, 14], Wissbrun [17–19, 23, 24], Wong [20], Mackley [66, 67] and Asada [68]. These models help to explain the low shear-rate region of shear thinning of viscosity and the dependence of texture and rheology on shear history. Thus the nature of the polydomain fluid [68] is critical to an understanding of the solid state textures of LCPs. It is the long relaxation times of such LCPs [24] that provide fruitful research in the evaluation of the textures frozen into the solid state.

Observation of small molecule liquid crystals in polarized light is known to reveal textures which are useful for identification of phase structures [69, 70]. PLM is useful for observation of liquid crystal domain textures both in dynamic studies, using a hot stage, and in the solid state. Nematic domains, characteristic of highly oriented thermotropic LCPs, can be observed in a polarized light micrograph of a LCP thin section (Fig. 1). The PLM image, which is viewed orthogonal to the crossed polarizers, reveals incomplete extinction and an elongated domain texture. Incomplete extinction is unexpected for a material such as a LCP, which is well oriented parallel to either polarization direction [38]. Furthermore, incomplete extinction is also observed for the aramid fibres [38] in which the textures observed are thought to be due to their sharp pleated sheet structure [71].

Nematic domains (Fig. 1) were observed in the solid state to be oriented with the fibre axis and exhibited polarization colours in the same order due to their similar orientation. Slight variations in colour suggested the presence of small orientation differences within the plane of the 1 μm thick section, accounted for by a serpentine trajectory or meander of the molecules [38]. A lateral banded texture was also observed in the solid state core of poorly oriented extrudates [38] and for many model studies in which the LCPs were sheared for sample preparation [49, 72, 73]. This banded texture, probably analogous to the pleated structure of the aramids, was interpreted by Donald and Windle [49, 72, 73] as being associated with a serpentine path of the molecules about the shear direction. The analogy to the meander reported for poly(*p*-phenylene benzobisthiazole) (PBZT) [31] and the sharp path caused by the pleated sheet structures of some Kevlar fibres [42] are all consistent. According to Zachariades *et al.* [71] the optical banded textures form in sheared LCPs by ordering of domains. Recent studies have confirmed the serpentine meander of the molecules and it is likely that the diffuse dark zones outlining the domains as shown by TEM are domain walls [49, 50]. Anwer *et al.* [53] suggested that these boundaries are analogous to the walls observed for small-molecule liquid crystals [69, 70].

A periodicity of about 500 nm has been reported for the banding and pleated textures observed for the aramids and copolyesters [6, 38, 42, 45, 48, 72, 73]. This dimension is consistent with the approximate 500 nm domain size observed in highly oriented thermotropic LCPs, as illustrated in Fig. 1. The lateral

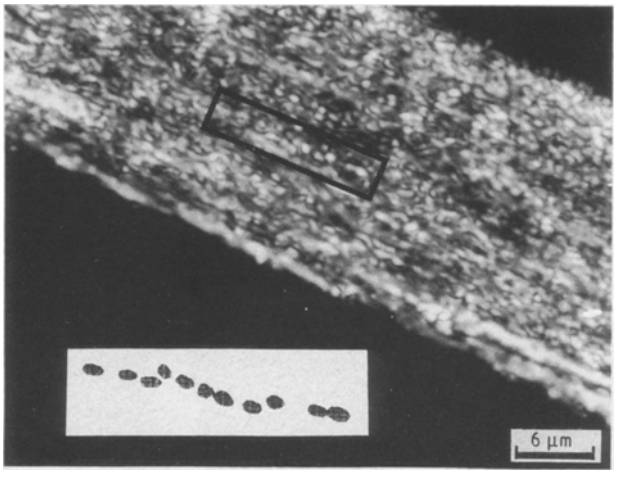

Figure 1 Polarized light micrograph, taken in the orthogonal view, of a thin section of a highly oriented Vectran tape showing domains elongated with the extrusion axis. The inset is a schematic drawing of the domains in the box suggesting they are a fibril meandering in and out of the plane of the section.

banded textures exhibited by some of the thermotropes and the pleated sheet textures exhibited by some of the aramids, as discussed above, are observed for those materials which have a poorer degree of molecular orientation. In fact, the more highly oriented thermotropic and lyotropic fibres do not exhibit these textures. For instance, in the case of the thermotropic copolyesters, the highly oriented heat-treated fibres do not exhibit any lateral banding. Likewise, Kevlar 149 exhibits higher modulus than Kevlar 49 [74], which is consistent for a material with increased crystallinity and crystallite size, and without a pleated sheet structure. The relationship of the domains to the fibrillar textures is also important. The inset in Fig. 1 is a magnified view of the polarized light micrograph of the Vectran tape on which is sketched the domains that appear to be aligned along the fibre axis. The schematic drawing shows that the worm-like domains consist of fibrils which meander in and out of the plane of the section, parallel to the director or fibre axis. The wall boundaries result, in part, from their homeotropic alignment.

3.2. Liquid crystal polymer fibrils

To interpret images obtained from new imaging techniques, similar materials must be explored using imaging methods that are well understood. Therefore, the LCPs were examined by SEM, FESEM and TEM for surface and bulk or internal detail prior to evaluation by STM. Representative complementary images are given in this paper and elsewhere [56, 57].

A fibrillar texture is observed for many LCPs including the thermotropes [38–40], aramids [6, 9, 38], and the "rigid-rod" polymers [25, 29, 31]. SEM images, acquired from Vectran fibres are presented in Fig. 2. The fibrils for less well oriented, large extrudates, can be highly woody in texture (Fig. 2a). A finer texture is exhibited for fibres with smaller micrometre-sized diameters (Fig. 2b, c). The peel-back technique clearly reveals the fibrillar nature of the fibre core (Fig. 2b, c). In contrast, the fibre surface tends to be smooth in texture (Fig. 2d). A common manifestation of this highly oriented texture is poor compressive properties, demonstrated by the kink bands in the SEM images acquired from the surface (Fig. 2d) and internal structure (Fig. 2e) of a fibre. The fracture mechanism in fatigue also reflects poor compressive properties [75–79]. Kink bands have been studied by Dobb *et al.* [79] for the aramids and a mechanism for their formation, consistent with tensile loss, was proposed. However, only conjecture has been made as to the primary cause of compressive failure. It is clear

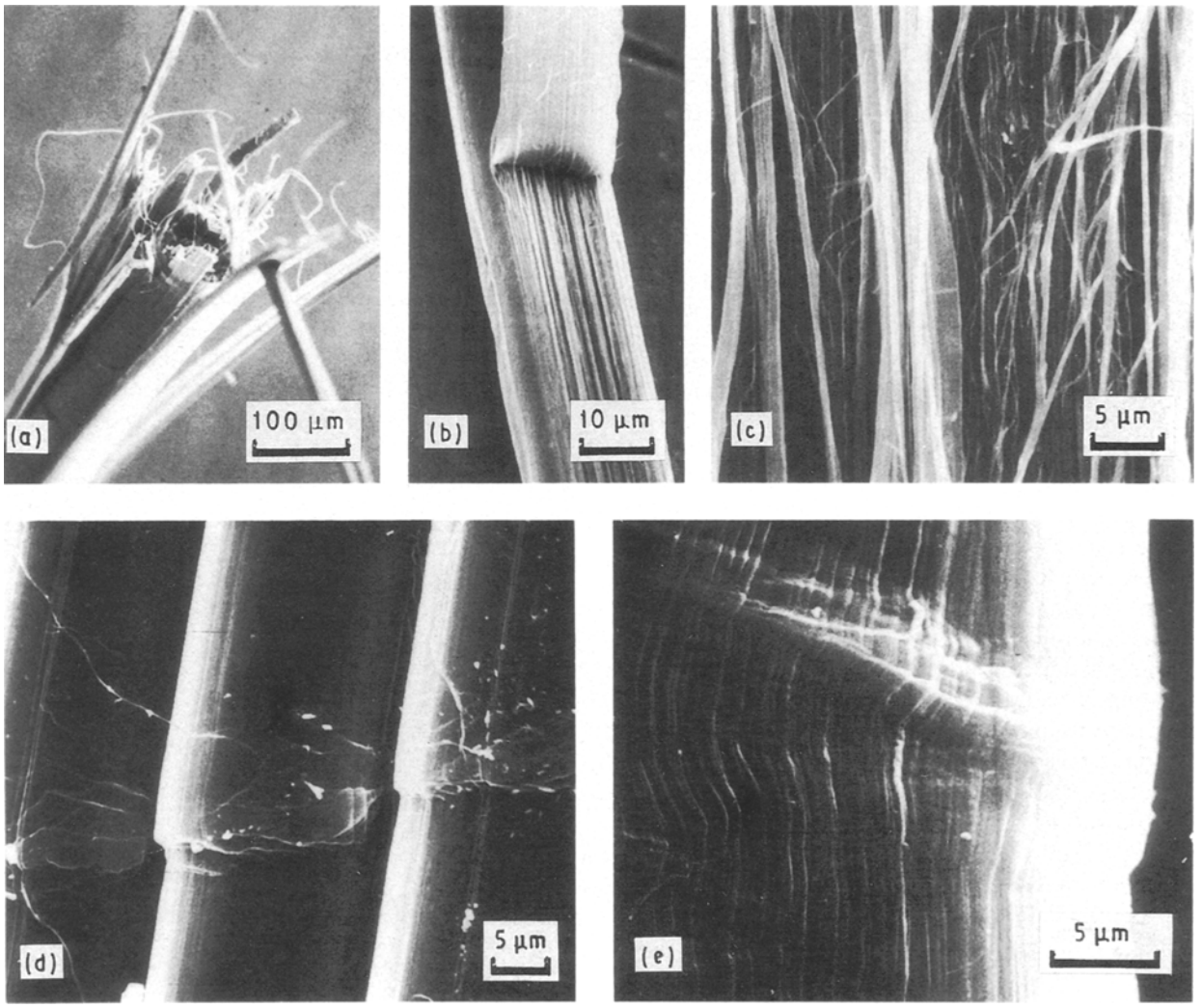

Figure 2 (a) Scanning electron micrographs reveal the woody nature of Vectra extrudates. (b, c) Images of peel back Vectran fibres show a fibrillar texture (d, e). The surface of the fibres is smooth with some discontinuities due to kink bands.

that kink bands are related to the deformation process but the size scale of its origin (fibre, fibril or microfibril) is uncertain. This topic will be discussed below.

FESEM images were acquired from highly oriented Vectran fibre which was peeled to reveal kinked regions (Fig. 3a). The highly ordered Vectran fibrillar structure also shows local deformation in the region of a kink band. A more ordered fibrillar organization is apparent for fibres after heat treatment (Fig. 3b) and for a Kevlar fibre (Fig. 3c) which also exhibits a fibrillar internal texture.

Peeled-back, highly oriented Vectran fibres and tapes were also imaged in the STM to explore details of the fibrillar and kink-band textures [56, 57]. Three-dimensional views are shown in the centre of Fig. 4a and b and top down views are shown in the lower right corners and in Fig. 4c and d. In the figure, the region scanned was 500 nm, along both the x and y axes, while the maximum z-axis range was about 50 nm. The organization of the fibrils and microfibrils is clearly detailed (Fig. 4) and local order can be compared to the typical bulk average order or orientation provided by X-ray analysis. The alignment of the microfibrils to the fibre axis is seen to be very good over all. Two types of local disorder are evident, however, especially in the top down views (Fig. 4c, d). The first type of disorder observed is the kink band in which there are clear discontinuities across the individual microfibrils (Fig. 4c, d) as well as damage to individual microfibrils (Fig. 4b, d). The STM images definitively revealed that damaged microfibrils are observed in shear bands which result from compressive damage and thus result in tensile strength loss. The second type of disorder observed is the "Y" shaped regions, where microfibril contours disappear beneath the surface (Fig. 4b). Although such structures were implied in the two-dimensional sections imaged by TEM (e.g. [35, 38]), the STM images provide important three-dimensional confirmation of microfibril organization. From STM images, direct measurements can be made of the fibril width and thickness. Therefore, their organization can be directly measured instead of inferring the third dimension from two-dimensional images.

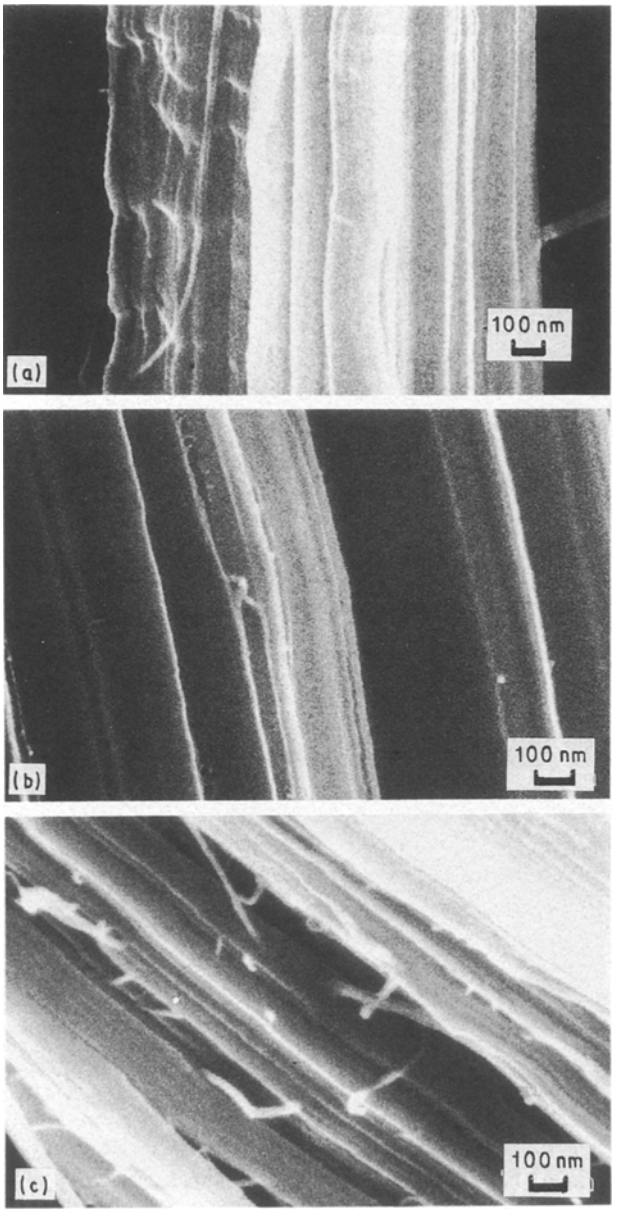

Figure 3 FESEM micrographs showing the internal texture in peeled-back highly oriented (a) Vectran as-spun, (b) Vectran heat-treated and (c) Kevlar fibres.

Although X-ray analysis demonstrates a high average orientation for LCP materials, microanalysis imaging techniques reveal that the local order is not uniform. Further observations of microstructure may provide a better understanding of process histories and mechanical properties.

3.3 Microfibrillar textures in LCPs

The three-tiered fibrillar hierarchy is a well-accepted LCP model with predictive import [38–40]. The current work using new high-resolution instruments permitted the observation of all the various size scales in one imaging device and led to our reconsideration of the hierarchy. There has always been some question whether microfibrils originated because of deformation during sample preparation, or whether they are an original form of structure within the nematic domains in the melt. Additionally, a question remains regarding the interaction of microfibrils within the LCPs and the effect on mechanical properties. It is these issues that are being investigated once again in the present study.

The sonication procedure, originally developed by Dobb *et al.* [41], and adapted by us [38], was used to prepare samples of Kevlar, and various Vectran fibres and highly oriented tapes for TEM imaging. TEM images of the sonicated materials (Fig. 5) clearly show a range of fibrillar sizes resulting from this preparation method. The fibrils are very long and tend to fibrillate into ever smaller units. However, no clear interfibril tie fibrils were observed by the high-resolution imaging methods. Twisting of the microfibrils is clearly shown in the three-dimensional images and in TEM (Fig. 5a) where the twist in a tape-like fibril is reminiscent of cellulosic fibres. In Fig. 5b, Kevlar is shown to fibrillate into units less than 10 nm wide. Similar-sized microfibrils are also observed within these fibrils. Fibril width and/or thickness measurements were

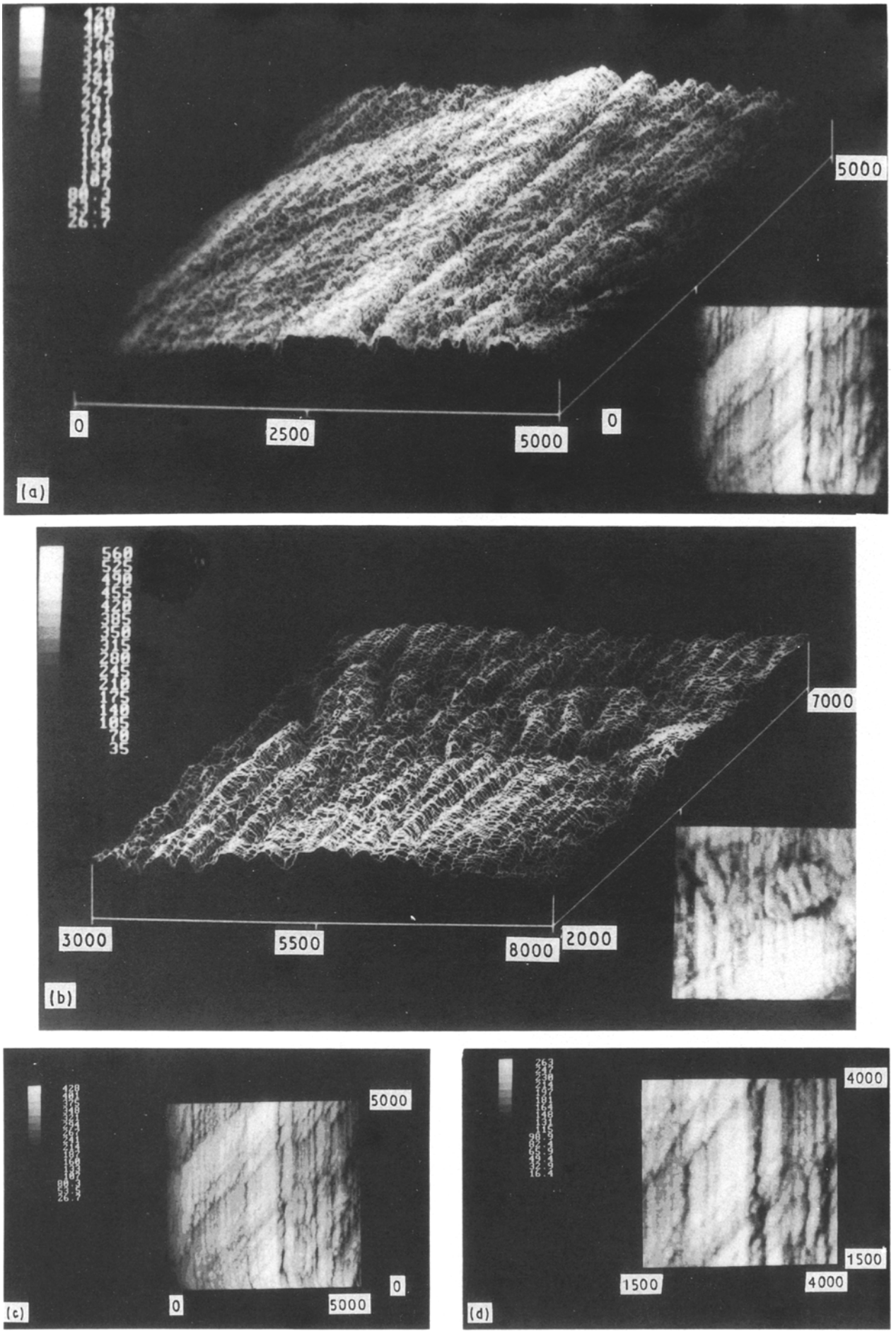

Figure 4 (a, b) STM micrographs of peel-back Vectran fibres in which fibre and microfibril orientation is vertical. Three-dimensional views (centre) accentuate z-height details; maximum z-height ($\sim$ 50 nm) divided into 15 grey levels. Top down views in lower right-hand corner (a, b) are shown in more detail in (c, d). Kink bands at an angle to the fibre axis are observed in all the images; individual broken microfibrils are observed in the region of the kink bands (b). Numerical values for scanned regions are in Ångstroms.

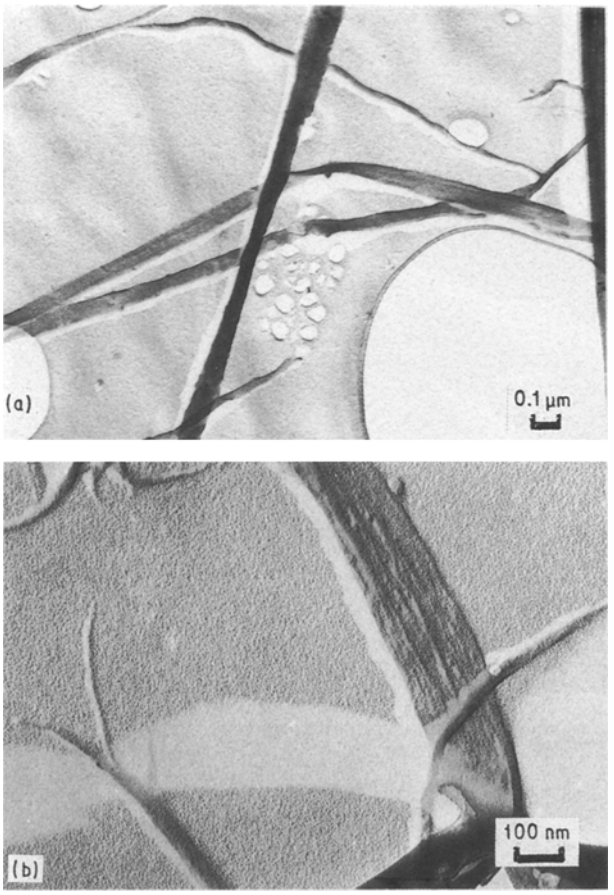

Figure 5 Transmission electron micrographs of sonicated fibrils of (a) Vectran and (b) Kevlar illustrating tape-like structure. Finer structures are observed to form due to fibrillation (a, b) but the fact that they are present within the larger fibrils (b) shows they exist within the spun fibres.

made using shadowing techniques [40] carefully controlling distances and angles in the vacuum evaporator. This tape-like structure is consistently observed in TEM studies of fibrils and microfibrils in all the LCPs studied.

Sonicated LCP samples were also imaged by STM to determine the dimensions of the smallest fibrils present in Vectran and Kevlar fibres with differing tensile modulus properties. In addition, evidence was sought related to the hierarchy and the genesis of the microfibrils. Early STM images, taken using the Nanoscope I, are shown in Fig. 6 [56] and recent STM images taken using the Nanoscope II are shown in Figs 7 and 8.

An overview of the sonicated fibrils (Fig. 6a) which shows large and small layered structures in three dimensions, looks remarkably similar to the TEM and FESEM views of the same sample. A more detailed view of the finer microfibrils in the Vectran sample (Fig. 6b) reveals two individual microfibrils. The width of the microfibrils is about 10 nm; the "thickness" (z height) of the microfibrils is about 3 nm. These measurements correspond to a tape-like structure, 3 nm by 10 nm, rather than a round fibrous shape.

STM images, taken with the Nanoscope II, of Vectran (Fig. 7) and Kevlar (Fig. 8) are more revealing. Each image series was acquired from the same area of the specimen, although smaller and smaller regions within each area were consecutively scanned, resulting in a series of images at successively higher magnifications. Fig. 7a and b show the nature of the coarser fibrils and reveals the microfibrils within these larger units. The microfibrils can be observed within the larger fibrils in the STM images acquired from both the as-spun Vectran (Fig. 7a) and heat-treated Vectran (Fig. 7b). Detailed views of the images in Fig. 7b are shown in more detail in Fig. 7c–e. A periodic texture is observed across a group of microfibrils arranged normal to the microfibril axis. It is very interesting to note that the periodicity of this texture is about 50 nm.

The series of STM images of Kevlar (Fig. 8) most clearly reveal the nature of the LCP hierarchy. Fig. 8a shows a bundle of uniform microfibrils, 10 nm wide within a larger aggregated fibrillar structure unit. The fine microfibrils can be observed more clearly in Fig. 8b–d. Finally, the on-line image analysis capability of the Nanoscope II permitted the measurement of the width and thickness of the smallest microfibrils (Fig. 8e). Many measurements were made of the finest microfibrils in Vectran and Kevlar fibres using this direct image measurement ability. The distribution of fibril width, thickness and the aspect ratio of width to thickness are shown in frequency histograms (Fig. 9) to reveal very similar dimensions for these very different fibre types, although the actual sizes are somewhat smaller for Kevlar than Vectran. Interestingly, the very smallest microfibril widths are on the order of 10 nm and the range is from 10–40 nm. The mean thickness of the microfibrils is about 3–5 nm and the smallest microfibrils are about 1 nm thick. It is clear from the measurements and the shape ratio considerations that the microfibrils are long and tape-like in shape as they are on the order of six to ten times as wide as they are thick.

3.5. LCP structure model

An extended structural model of the LCP hierarchy which is the culmination of these microscopy studies is presented in Fig. 10. This new model further elucidates the microfibrillar sizes and shapes first described in the earlier model [38–40] thereby providing a detailed description of the LCP structural features from the macromolecular to nanomolecular size scale. The model once again confirms the presence of a hierarchy, specific to the liquid crystalline polymers. The key microstructural element responsible for the properties of these thermotropic and lyotropic LCPs is the microfibril, the same microstructural unit basic to melt-spun and drawn flexible polymers. The tape-like shape of the microfibril and its size support the basic two-chain molecular organization that has been proposed by Ward and co-workers [61, 80] and Windle [81] in which the size of the smallest microfibrils are ~ 1 nm.

Important features of the original model that have been confirmed in the present work relate to the organization and size of the microfibrils. The orientation of the microfibrils and the bundles collected as

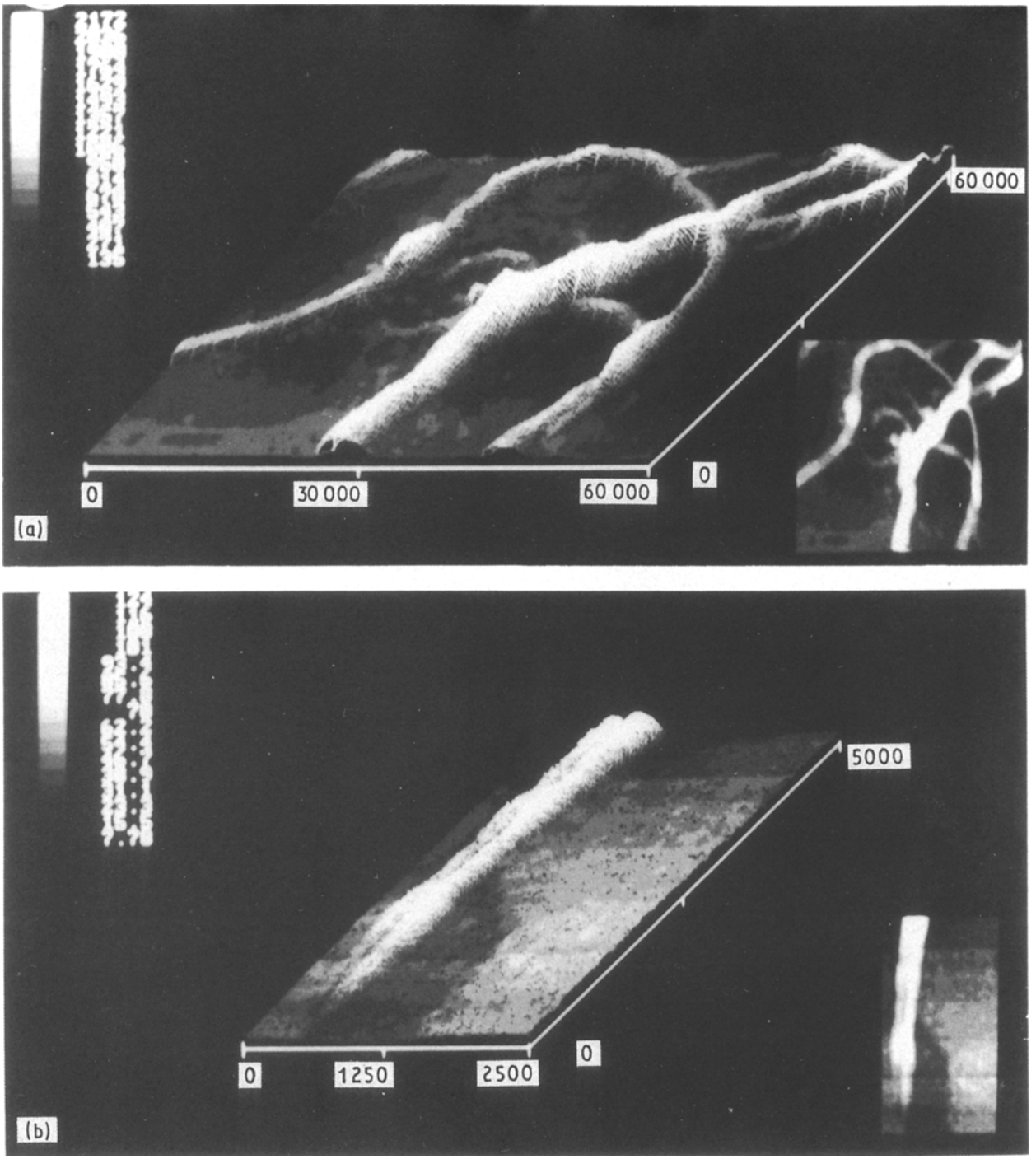

Figure 6 STM images of sonicated Vectran fibrils are observed in (a) a 6 μm × 6 μm overview image, and (b) in more detail in a 250 nm × 500 nm image. The detailed image (b) reveals two microfibrils ~ 10 nm wide and about 3 nm thick (z dimension). Numbers on the image are in Ångstroms.

fibrils is generally along the fibre or elongational axis. However, on a local scale it is clear that the microfibrils meander along the path of the director and are not best represented by a stick-like rigid-rod scheme, but rather are best characterized as worm-like in nature, somewhere between the random coil model of conventional polymers and the true rigid-rod structures. These worm-like microfibrils meander in and out of the plane of the director as shown by the "Y" shaped junctions in many of the images. The microfibrils are flat in shape and tend to layer readily without the need of tie fibrils. Although, there is a range of fibril and microfibril sizes, the smallest stable structures are shown in the model. A more complete discussion of the model and its implications is described below.

4. Discussion

In the last decade, major technological developments have occurred for the production of polymer fibres with high mechanical strength and stiffness. In concert with these efforts, studies have been directed towards a better understanding of the relationship between chemical composition, physical structure and mechanical properties. One goal is to develop a predictive structure–property model which can result in the development of improved marketable technologies.

For highly oriented thermotropic and lyotropic liquid crystalline fibres, there are a series of questions that must be answered to determine whether there is one consistent structural model. They are:

(a) What is the supramolecular nature of liquid crystalline polymers?
(b) Does a hierarchy of structures exist and what is its nature?
(c) Can such a hierarchy be generalized for both lyotropic and thermotropic liquid crystalline polymers?
(d) What is the three-dimensional size and shape of the microfibril?
(e) Does the size and/or the organization of the microfibril relate to the stiffness of the fibrous product?

Polarized light microscopy revealed domains of micrometre-sized structures in the thermotropic LCPs aligned along the fibre axis. The domains in the solid state were consistent with nematic domains thought to be discrete entities in the nematic melt or solution [11–13, 17–20, 23, 24]. The meander of the domains was shown (Fig. 1) to be consistent with their polarization colours. Fibrils pulled out of the same oriented specimen consisted of fibrils, oriented along the fibre axis, with the same width as the domains. Models have suggested that the organization is such that the domains consist of fibrils which are further composed of smaller microfibrils. The presence of domain walls appears to be consistent with the worm-like arrangement of the fibrils in and out of the plane of the section. This meander is further illustrated in the three-dimensional STM images. Highly aligned fibrils exhibit a shallow trajectory as they meander through highly oriented fibres and films. Thus the organization of the thermotropic LCPs appears to include microfibrils arranged within fibrils.

Sonicated fibres were presented in earlier TEM images [35, 38–40] ; however, the present study reveals for the first time that microfibrils definitely exist within the larger fibrillar units. The fibrils clearly pull apart and there is no indication of tie fibrils holding them together. Additionally, the shape of the fibrils and microfibrils appears to be flat or tape-like and some twisting of the fibrils is observed. The most definitive images, however, are those of sonicated Vectran and Kevlar fibrillar structures shown in the STM images (Figs 7 and 8). For the first time, all of the hierarchical structures are delineated clearly in the same region of the material. Large fibrils, ~ 0.5–$1\ \mu m$ across, are seen to consist of smaller and smaller microfibrils. Microfibrils about 10 nm across are shown to be well aligned within a larger fibril. Detailed images show that the smallest microfibrils range in size from 3–30 nm wide and from 2–5 nm thick. These numerical values suggest that the three-dimensional microfibril shape is tape-like. The image detail is of sufficient quality in the 1–10 nm range that histograms of the microfibrillar width and thickness provide comparison of the microfibril size for polymers of different compositions and heat treatments. Studies thus far suggest that the microfibril sizes and shapes are similar for lyotropic and thermotropic LCPs, as well as for as-spun and heat-treated fibres.

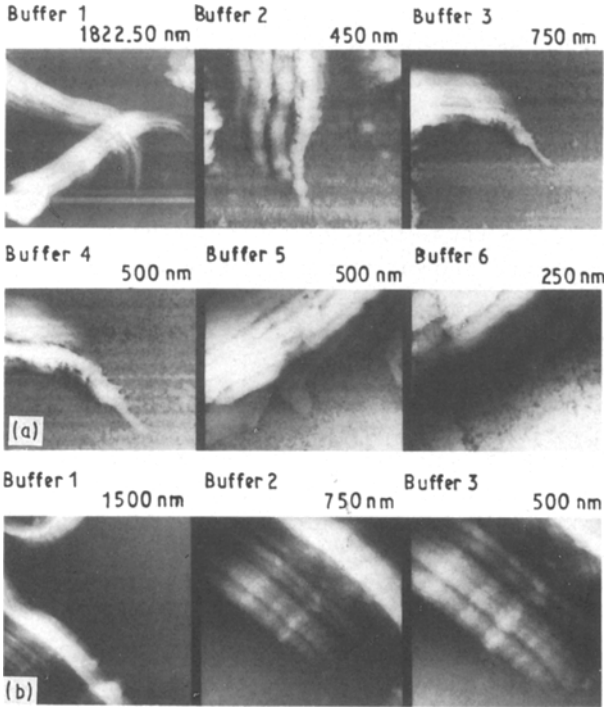

Figure 7 STM images of Vectran (a) as-spun and (b) heat-treated reveal a range of fibrillar sizes in images scanned at successively higher magnifications. The images in (b) are shown in more detail (c–e) to consist of finer microfibrils within larger fibrils. Lateral banded textures (c–e) reveal a 50 nm periodicity.

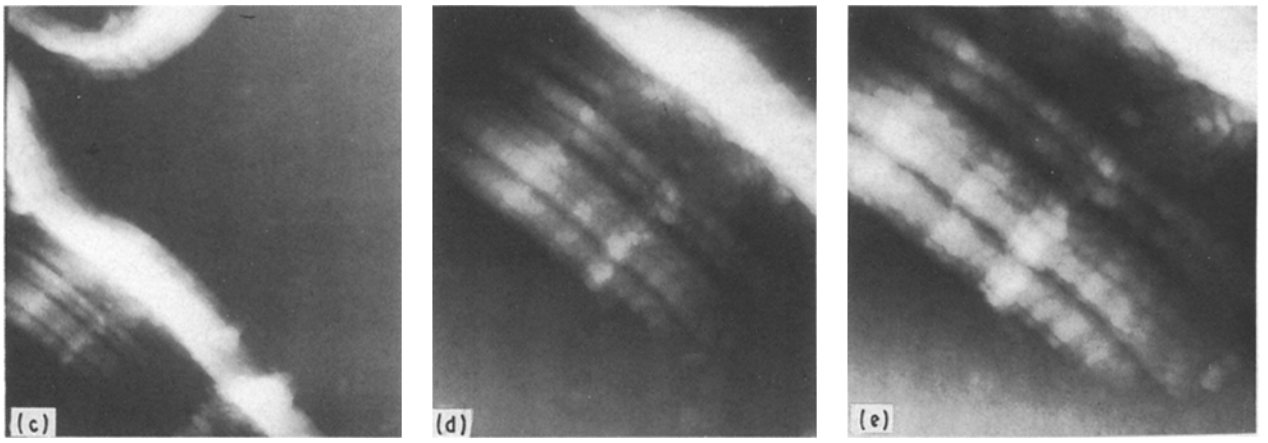

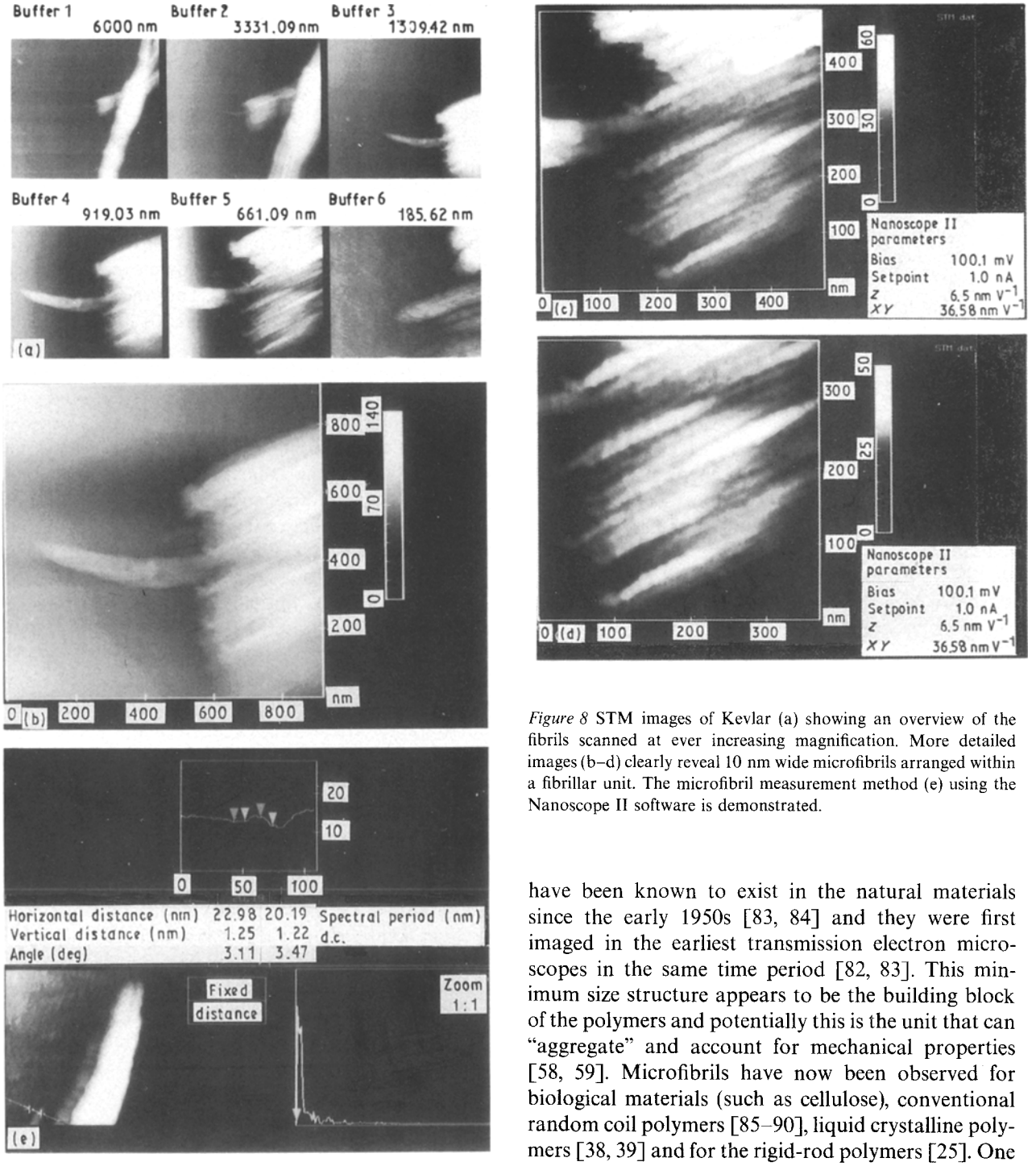

Figure 8 STM images of Kevlar (a) showing an overview of the fibrils scanned at ever increasing magnification. More detailed images (b–d) clearly reveal 10 nm wide microfibrils arranged within a fibrillar unit. The microfibril measurement method (e) using the Nanoscope II software is demonstrated.

Although the microfibrils and fibrils are, on average, oriented with the fibre axis, in agreement with X-ray diffraction studies (e.g., [25, 36, 48–55]), they are not perfectly uniform and oriented on a local scale. In fact, the STM, TEM and FESEM images obtained from the *in situ* structures suggest that the fibrils weave or meander in and out of the longitudinal plane and exhibit a worm-like trajectory rather than a "rigid-rod" structure, as generally portrayed for the nematic LCPs.

One general concept that has received much attention is the notion that the microfibril is the fundamental building block in polymers made from flexible linear molecules. A decade ago Sawyer and George [82] proposed a basic microfibrillar building block for both natural and synthetic materials. The microfibrils have been known to exist in the natural materials since the early 1950s [83, 84] and they were first imaged in the earliest transmission electron microscopes in the same time period [82, 83]. This minimum size structure appears to be the building block of the polymers and potentially this is the unit that can "aggregate" and account for mechanical properties [58, 59]. Microfibrils have now been observed for biological materials (such as cellulose), conventional random coil polymers [85–90], liquid crystalline polymers [38, 39] and for the rigid-rod polymers [25]. One factor that appears similar for materials as dissimilar as cellulose, polyesters, lyotropic aramids and thermotropic liquid crystalline polymers is that the general shape of the molecular chain is rather long compared to its width and thickness. Thus it is possible that the microfibril is simply a replication of the molecular chain. This replication, and the straightness of the chain, is dependent upon the specific chemical composition. The association of chains into microfibrils and the aggregation of microfibrils into fibrils suggests that the microfibril might be the smallest structure associated with mechanical properties.

The extended, worm-like nature of the microfibrils is consistent with the generally high orientation values calculated from X-ray diffraction results. However, these orientation values are very high and they do not exhibit significant variations even for fibres with quite different tensile modulus. Ward [80] has stated that

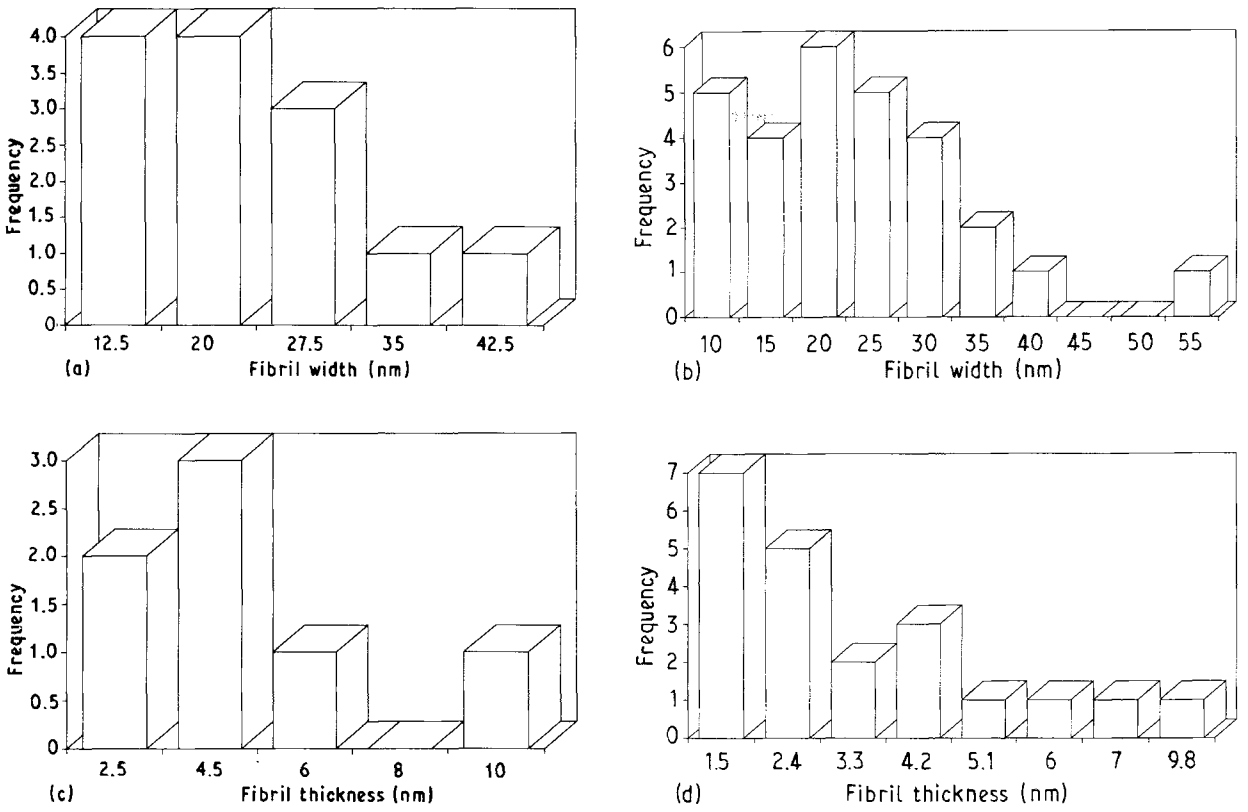

Figure 9 The distribution of the width and thickness of microfibrils in Vectran and Kevlar shown in histogram format; measurements were made directly from STM images. The mean of the fibril widths for (a) Vectran and (b) Kevlar are about 22 nm, with a standard deviation (breadth of the distribution) of about 10 nm. The mean of the fibril thickness for (c) Vectran and (d) Kevlar are about 5 and 3 nm, respectively, with standard deviations about 2.5 nm. Thus the thickness values are very similar, as are the fibril widths. The width to thickness ratios are about 6–8 for both fibre types.

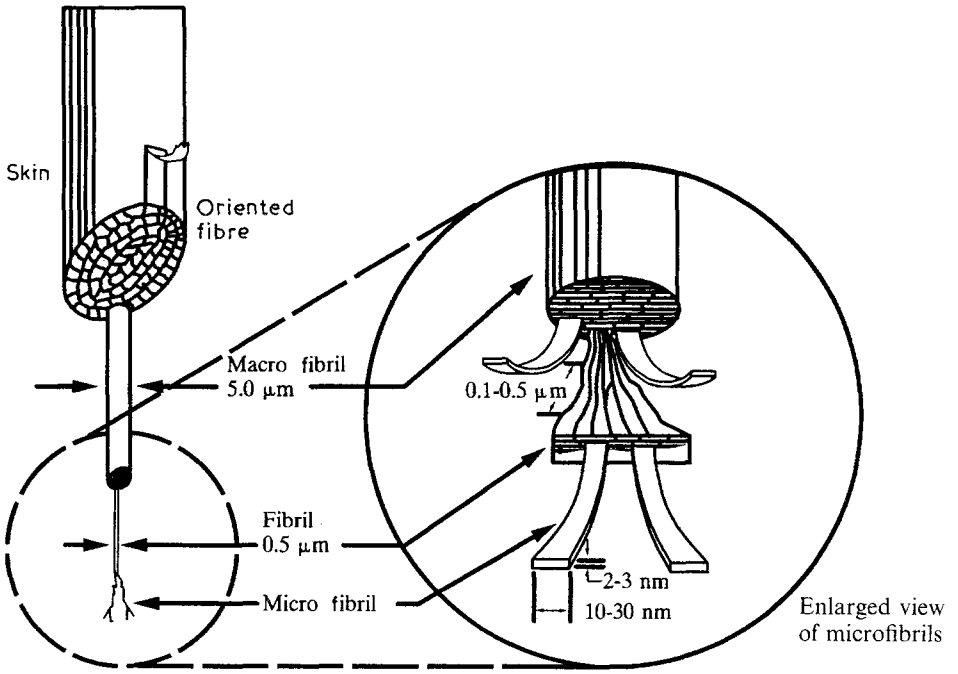

Figure 10 An expanded structural model is shown for the thermotropic and lyotropic LCPs, with more detail of the microfibril sizes, shapes and order.

X-ray diffraction does not provide the complete answer for understanding the tensile modulus properties of the LCPs. In the case of the aramids, with a true three-dimensional structure, the X-ray results, combined with the presence or absence of the pleated sheet structure, are consistent with lower and higher tensile modulus or stiffness values, respectively. In fact, the higher modulus aramid variants exhibit about 80% –90% of theoretical tensile modulus values [74] when there is no pleated structure. Chain rigidity and strong intermolecular cohesive forces in the solid state, owing to hydrogen bonding [91] are responsible for these

properties. Thus the "straightness" of the extended-chain structure imposed by the chemical composition and the processing are related to the range of tensile moduli observed. It is interesting to note that two polymorphs have been observed for the aramids [92, 93] with the pseudo-orthorhombic structure exhibiting two chains per unit cell. This is similar to the work of both Ward and co-workers [61, 80] and Windle [81] who suggest the same two-chain structure for the thermotropes. In both cases, the size of the two-chain fundamental unit is ~ 1 nm, the size of the smallest microfibril.

The final mechanical parameter of interest, although one which is known to be poor for these highly oriented materials, is compressive strength. Intuitively, low compressive strength seems consistent with a highly oriented texture, although the mechanism of compressive failure is not fully known. What is known is that kink bands form in the thermotropes and the aramids, as was shown in Figs 2 and 3. It has not been shown previously whether failure at these kink bands is macroscopic in natûre or occurs on a smaller scale. The figures in this study reveal, for the first time, that the early onset of compressive failure, associated with kink band formation, results in failure on the microfibril size (2–10 nm) scale. When a significant number of these microfibrils are severed the kink band must open up, resulting in failure. More work is needed to understand fully the stress transfer method implied by these observations, but the results strongly suggest that the mechanical building block is the microfibril and that they can fail individually.

Rigid-chain polymers, i.e. all LCPs, follow the aggregate model [2, 4, 58–61] whereas a composite model with tie molecules, crystalline bridges and long crystals is better for highly oriented flexible polymers such as polyethylene [80]. The high mechanical properties of the aramids are thought to be associated with chains in crystallographic registry, i.e. the persistence length of the molecular chain is greater than the average axial distance between the crystallites. The best mechanical properties are associated with aramids which do not exhibit the axially periodic defect layer. In a consistent manner, the thermotropes with the best mechanical properties do not exhibit the lateral banded texture, suggesting that better molecular chain registry is associated with improved properties. However, the lack of three-dimensional crystallographic registry in the Vectran fibres does not preclude similar overall properties compared to the aramids. Thus three-dimensional crystallinity, and the tie molecules associated with the extended-chain polyethylenes and aramids, are not required for high performance.

The question of interfibrillar stress transfer has not been fully resolved. There were five possible mechanisms proposed earlier [38] for interfibrillar stress transfer, of which only three now still appear to be possible and consistent with the current observations. The possible mechanisms appear to include:

1. A fibrillar network, as hypothesized by Allen *et al.* in PBZT [29] ;
2. Interfibrillar friction due to the tortuosity and proximity of fibrillar units, as hypothesized by Sawyer and Jaffe [38] ;
3. Interchain interactions–strong evidence points to chain slippage as the ultimate failure mechanism (see Yoon [37]).

The expanded structural model presented appears to be consistent with interactions among the microfibrils due to their tortuosity and proximity. These local interactions and the variation of the tortuosity or organization of the microfibrils among samples with different tensile properties is likely to be important in understanding the mechanism of mechanical property limitations. Further study is required to understand how the size and organization of the microfibrils and the entire hierarchy relate to the tensile strength and tensile modulus of these high-performance LCPs.

5. Conclusions

The conclusions of this work confirm and expand on those ideas in earlier papers by Sawyer and Jaffe [38, 39], and Sawyer *et al.* [40, 56, 57]. All LCPs studied to date are composed of the same fibrillar building blocks arranged in a hierarchy reminiscent of biological systems such as collagen and cellulose. The microfibrils are tape-like in shape and this is hypothesized to be due to a replication of the rod-like molecular chain. Comparison of the molecular and microfibrillar sizes suggest that the microfibrils are composed of a minimum of two molecules, in the smallest dimension, and thus they represent the finest nanostructural element in the LCPs. An extended LCP structural model, consisting of well-ordered, elongated fibrils, continues to be consistent with measured properties: high anisotropy, very high tensile modulus and tensile strength, and poor shear and compressive properties in the lateral dimension.

For the first time, evidence has been shown which suggests that the microfibril is the finest unit which mediates mechanical properties, including compressive strength and tensile modulus. A major conclusion of this work is that the sizes of the microfibrils appear similar for all the lyotropic and thermotropic LCPs studied. Thus, the microfibrillar sizes are not very different for fibres with different tensile strength values, such as before and after heat treatment, or for fibres with different tensile modulus values. However, the organization of the microfibrils does appear to differ with tensile modulus, as the higher degree of local order, improvements in lateral arrangement and orientation all reflect higher tensile modulus values. The nature of the nanostructural, microfibrillar units, meandering through otherwise highly oriented LCPs, is being used to understand further the origin of mechanical properties.

Questions remain regarding the nature of the transformations occurring during heat treatment and the nature of the tensile strength failure mechanism. In addition, the interfibrillar stress transfer mechanism is still not known.

Acknowledgements

The present work was initiated as a result of stimulating discussions and collaboration with Michael Jaffe and Larry Charbonneau of Hoechst Celanese. The study was made possible by the on-going collaboration between Hoechst Celanese and North Carolina State University. Extremely helpful discussions with Ian Ward (Leeds University), Alan Windle (Cambridge University) and colleagues in Hoechst Celanese, notably Michael Jaffe, Gerry Farrow and Hyun-Nam Yoon, are all gratefully acknowledged. The authors would like to acknowledge Howard Furst and Greg Nelson for computer generation of the model, the X-ray diffraction studies of Paul J. Harget and Cheng K. Saw and to thank Tom Bruno for the sample preparation. Finally, thanks to the management of Hoechst Celanese for support of our research. The support of Hoechst Celanese is gratefully acknowledged (I.H.M., P.E.R.) for their sponsorship as part of the NSF PYI program (P.E.R.), and to N.S.F for support (P.E.R., I.H.M.) under contract DMR-8657813.

References

1. G. CALUNDANN and M. JAFFE, in "Proceedings of The Robert A. Welch Conferences on Chemical Research XXVI", Synthetic Polymers, Houston, Texas, 15-17 November 1982, p. 247.
2. G. R. DAVIES and I. M. WARD, in "High Modulus Polymers", edited by A. Zachariades and R.S. Porter (Marcel Dekker, New York, 1988).
3. A. ZACHARIADES and R. S. PORTER (eds), "The Strength and Stiffness of Polymers" (Marcel Dekker, New York, 1983).
4. *Idem*, "High Modulus Polymers" (Marcel Dekker, New York, 1988).
5. A. CIFERRI, W. R. KRIGBAUM and R. B. MEYER (eds), "Polymer Liquid Crystals" (Academic Press, New York, 1982).
6. M. G. DOBB and J. E. MCINTYRE, in "Advances in Polymer Science 60/61" (Springer-Verlag, Berlin, 1984).
7. S. L. KWOLEK, US Pats 3600 350 (1971) and 3671 542 (1972).
8. H. BLADES, U S Pat. 3767 756 (1973).
9. M. PANAR, P. AVAKIAN, R. C. BLUME, K. H. GARDNER, T. D. GIERKE and H. H. YANG, *J. Polym. Sci. Polym. Phys. Ed.* **21** (1983) 1955.
10. M. JAFFE and R. S. JONES, in "High Technology Fibers", Part A, "Handbook of Fiber Science and Technology", Vol. III, edited by M. Lewin and J. Preston (Marcel Dekker, New York, 1985).
11. L. ONSAGER, *N.Y. Acad. Sci.* **51** (1949) 627.
12. A. ISIHARA, *J. Chem. Phys.* **19** (1951) 1142.
13. P. J. FLORY, *Proc. Roy. Soc.* **A234** (1956) 73.
14. *Idem*, in "Polymer Liquid Crystals", edited by A. Ciferri, W.R. Krigbaum and R.B. Meyer (Academic Press, New York, 1982).
15. Y. IDE and Z. OPHIR, *Polym. Engng Sci.* **23** (1983) 261.
16. Z. OPHIR and Y. IDE, *ibid.* **23** (1983) 792.
17. K. F. WISSBRUN, *Brit. Polym. J.* **12** (1980) 163.
18. *Idem*, *J. Rheol.* **25** (1981) 619.
19. K. F. WISSBRUN and A. C. GRIFFEN, *J. Polym. Sci. Polym. Phys. Ed.* **20** (1982) 1835.
20. C. P. WONG, H. OHNUMA and G. C. BERRY, *J. Polym. Sci. Polym. Symp.* **65** (1978) 173.
21. Z. TADMOR and C. G. GOGOS, "Principles of Polymer Processing" (Wiley Interscience, New York, 1979).
22. H. THAPAR and M. BEVIS, *J. Mater. Sci. Lett.* **2** (1983) 733.
23. K. F. WISSBRUN, *Farad. Discuss. Chem. Soc.* **79** (1985) 161.
24. K. F. WISSBRUN, G. KISS and F. N. COGSWELL, *Chem. Engng Commun.* **53** (1987) 149.
25. E. J. ROCHE, T. TAKAHASHI and E. L. THOMAS, in "Fiber Diffraction Methods", edited by A.D. French and K. H. Gardner, A. C. S. Symposium Series No. 141 (1980) p. 303.
26. J. R. SCHAEFGEN, T. I. BAIR, J. W. BALLOU, S. L. KWOLEK, P. W. MORGAN, M. PANAR and J. ZIMMERMAN, in "Ultra-high Modulus Polymers", edited by A. Ciferri and I. M. Ward (Applied Science, London, 1979) p. 173.
27. M. G. NORTHOLT, *Polymer* **21** (1980) 1199.
28. J. R. SCHAEFGEN, in "The Strength and Stiffness of Polymers", edited by A. Zachariades and R. S. Porter, (Marcel Dekker, New York, 1984) p. 327.
29. S. R. ALLEN, A. G. FILLIPPOV, R. J. FARRIS and E. L. THOMAS, *ibid.*, p. 357.
30. W. C. WOOTEN, Jr, F. E. McFARLANE, T. F. GRAY, Jr, and W. J. JACKSON Jr, in "Ultra-high Modulus Polymers", edited by A. Ciferri and I. M. Ward (Applied Science, London, 1979) p. 227.
31. E. J. ROCHE, R. S. STEIN and E. L. THOMAS, *J. Polym. Sci. Polym. Phys. Ed.* **18** (1980) 1145.
32. W. J. JACKSON Jr, and H. F. KUHFUSS, *J. Polym. Sci. Polym. Chem. Ed.* **14** (1976) 2043.
33. J. ECONOMY and W. VOLKSEN, in "The Strength and Stiffness of Polymers", edited by A. Zachariades and R. S. Porter (Marcel Dekker, New York, 1983) p. 293.
34. R. N. DeMARTINO, *J. Appl. Polym. Sci.* **28** (1983) 1805.
35. L. C. SAWYER, *J. Polym. Sci. Polym. Lett. Ed.* **22** (1984) 347.
36. J. B. STAMATOFF, *Molec. Cryst. Liq. Cryst.* **110** (1984) 75.
37. H. Y. YOON, *Colloid and Poly. Sci.* **268** (1990) 230.
38. L. C. SAWYER and M. JAFFE, *J. Mater. Sci.* **21** (1986) 1897.
39. *Idem*, in "High Performance Polymers", edited by E. Baer and A. Moet (Carl Hanser, Germany, 1991) p. 56.
40. L. C. SAWYER and D. T. GRUBB, "Polymer Microscopy" (Chapman and Hall, London, 1987).
41. M. G. DOBB, D. J. JOHNSON and B. P. SAVILLE, *J. Polym. Sci. Polymer Symp.* **58** (1977) 237.
42. *Idem*, *J. Polym. Sci.* **15** (1977) 2201.
43. M. G. DOBB, A. M. HENDELEH, D. J. JOHNSON and B. P. SAVILLE, *Nature* **253** (1975) 189.
44. S. C. BENNETT, M. G. DOBB, D. J. JOHNSON, R. MURRAY and B. P. SAVILLE, in "Proceedings EMAG 75" (Academic Press, Bristol, London, 1976) p.329.
45. M. G. DOBB, D. J. JOHNSON and B. P. SAVILLE, *Polymer* **22** (1981) 961.
46. R. HAGEGE, M. JARRIN and M. J. SOTTON, *J. Microsc.* **115** (1979) 65.
47. T. WENG, A. HILTNER and E. BAER, *J. Mater. Sci.* **21** (1986) 744.
48. C. VINEY, A. M. DONALD and A. H. WINDLE, *ibid.* **18** (1983) 1136.
49. A. M. DONALD and A. H. WINDLE, *ibid.* **18** (1983) 1143.
50. A. M. DONALD, *Phil. Mag.* **A47** (1983) L13.
51. A. M. DONALD and A. H. WINDLE, *J. Mater. Sci. Lett.* **4** (1985) 58.
52. *Idem*, *Polymer* **25** (1984) 1235.
53. A. ANWER, R. J. SPONTAK and A. H. WINDLE, *J. Mater. Sci. Lett.* **9** (1990) 935.
54. A. H. WINDLE, C. VINEY, R. GOLOMBOK and G. R. MITCHELL, *Farad. Discuss. Chem. Soc.* **79** (1985) 55.
55. G. A. GUTIERREZ, R. A. CHIVERS, J. BLACKWELL, J. B. STAMATOFF and H. N. YOON, *Polymer* **24** (1983) 937.
56. I. H. MUSSELMAN, P. E. RUSSELL, R. T. CHEN, M. G. JAMIESON and L. C. SAWYER, in "Proceedings of the XIIth International Congress for Electron Microscopy", Seattle, August 1990, edited by W. Bailey (San Francisco Press, San Francisco, 1990) p. 866.
57. L. C. SAWYER, R. T. CHEN, M. JAMIESON, I. H. MUSSELMAN and P. E. RUSSELL, *J. Mater. Sci. Lett.* **11** (1992) 69.
58. M. J. TROUGHTEN, A. P. UNWIN, G. R. DAVIES and I. M. WARD, *Polymer* **29** (1988) 1389.
59. D. I. GREEN, A. P. UNWIN, G. R. DAVIES and I. M. WARD, *ibid.* **31** (1990) 579.
60. D. I. GREEN, G. R. DAVIES, I. M. WARD, M. H. ALHAJMOHAMMED and S. ABSUL JOWAD, *Polym. Adv. Technol.* **1** (1990) 41.

61. R. A. ALLEN and I. M. WARD, *Polymer* **32** (1991) 203.
62. A. CIFERRI and B. VALENTI, in "Ultra-high Modulus Polymers" edited by A. Ciferri and I.M. Ward (Applied Science, London, 1979) p. 1.
63. D. J. BLUNDELL, *Polymer* **23** (1982) 359.
64. L. C. SAWYER, in "Proceedings of the 39th Annual Meeting of the EMSA", edited by G.W. Bailey (Claitors, Baton Rouge, 1981) p. 334.
65. I. H. MUSSELMAN and P. E. RUSSELL, in "Microbeam Analysis" edited by P. E. Russell, (San Francisco Press, San Francisco, CA, 1989) p. 535.
66. M. R. MACKLEY, F. PINAUD and G. SIEKMANN, *Polymer* **22** (1981) 437.
67. D. J. GRAZIANO and M. R. MACKLEY, *Molec. Cryst. Liq. Cryst.* **106** (1984) 73.
68. T. ASADA, in "Polymer Liquid Crystals", edited by A. Ciferri, W. R. Krigbaum, and R. B. Meyer (Academic Press, New York, 1982) p. 247.
69. P. G. de GENNES, "The Physics of Liquid Crystals" (Oxford University Press, 1979).
70. D. DEMUS and L. RICHTER, "Textures of Liquid Crystals" (Verlag Chemie, New York, 1978).
71. A. ZACHARIADES, P. NAVARD and J. A. LOGAN, *Molec. Cryst. Liq. Cryst.* **110** (1984) 93.
72. A. M. DONALD and A. H. WINDLE, *Coll. Polym. Sci.* **261** (1983) 793.
73. *Idem, J. Mater. Sci.* **19** (1984) 2085.
74. S. J. KRAUSE, D. L. VEZIE and W. W. ADAMS, *Polym. Commun.* **30** (1989) 10.
75. C. O. PRUNEDA, R. J. MORGAN, F. M. KONG, J. A. HODSON, R. P. KERSHAW and A. W. CASEY, in "Proceedings of the 29th National SAMPE Symposium", (1984) p. 1213.
76. J. H. GREENWOOD and P. G. ROSE, *J. Mater. Sci.* **9** (1974) 1804.
77. A. R. BUNSELL, *ibid.* **10** (1975) 1300.
78. M. H. LAFITE and A. R. BUNSELL, *ibid.* **17** (1982) 2391.
79. M. G. DOBB, D. J. JOHNSON and B. P. SAVILLE, *Polymer* **22** (1981) 1960.
80. I. M. WARD, private discussions.
81. A. H. WINDLE, private discussions.
82. L. H. SAWYER and W. GEORGE, in "Cellulose and Other Natural Polymer Systems: Biogensis, Structure, and Degradation", edited by R. Malcolm Brown Jr, (Plenum, New York, 1982) p. 429.
83. E. BAER and A. MOET (eds), "High Performance Polymers" (Hanser, New York, 1991).
84. A. FREY-WYSSLING, *Science* **119** (1954) 80.
85. A. PETERLIN, *J. Mater. Sci.* **6** (1971) 490.
86. *Idem, Polym. Engng Sci.* **18** (1978) 277.
87. *Idem*, in "Ultra-high Modulus Polymers", edited by A. Ciferri and I.M. Ward (Applied Science, London, 1979) p. 279.
88. B. KALB and A. J. PENNINGS, *J. Mater. Sci.* **15** (1980) 2584.
89. J. SMOOK, M. FLINTEMAN and A. J. PENNINGS, *Polym. Bull.* **2** (1980) 775.
90. *Idem, J. Mater. Sci.* **19** (1984) 31.
91. S. KWOLEK, W. MEMGER and J. E. VAN TROMP, in "International Symposium on Polymers for Advanced Technology", edited by M. Lewin, (International Union of Pure and Applied Chemistry, 1987) p. 421.
92. M. G. NORTHOLT, *Eur. Polym. J.* **10** (1974) 799.
93. K. HARAGUCHI, T. KAJIYAMA and M. TAKAYANAGI, *J. Appl. Polym. Sci.* **23** (1979) 915.

Received 3 February
and accepted 17 February 1992